

Infrared temperature measurement and increasing infrared measurement accuracy in the context of machining process

Masoudi, S.^{a,*}, Gholami, M.A.^b, Janghorban Iariche, M.^c, Vafadar, A.^d

^aYoung Researchers and Elite Club, Najafabad Branch, Islamic Azad University, Najafabad, Iran

^bDepartment of Mechanical Engineering, Shiraz Branch, Islamic Azad University, Shiraz, Iran

^cAbadan School of Medical Sciences, Abadan, Iran

^dSchool of Engineering, Edith Cowan University, Perth, Australia

ABSTRACT

One of the major challenges in the machining process is measuring the temperature accurately which has a considerable importance in calibrating finite element models and investigating thermodynamic of machining process. In the present paper, one of the effective methods for measuring temperature in the machining processes – i.e. infrared imaging – is used and effective parameters which increase measurement accuracy are investigated. One of the most effective parameter in the temperature measurement accuracy of infrared imaging is extracting and calibrating the emissivity coefficient for different temperature ranges. The obtained results show that the lack of precision calibration of the emissivity for different temperature ranges may cause high error in the measurement results. To measure temperature, several experiments are performed for turning a thin walled workpiece which is made of aluminium alloy Al-7075 and the effects of the machining parameters and tool material – polycrystalline diamond (PCD) and cemented carbide – are studied. Based on the achieved results, it can be concluded that the generated temperature in the cutting area can be decreased significantly by using PCD tools and selecting appropriate machining parameters.

© 2017 PEI, University of Maribor. All rights reserved.

ARTICLE INFO

Keywords:

Machining
IR temperature measurement
Emissivity
PCD tool
Carbide tool
Al-7075

*Corresponding author:

smasoudi86@gmail.com
(Masoudi, S.)

Article history:

Received 25 June 2017
Revised 14 October 2017
Accepted 20 October 2017

1. Introduction

In metal machining processes, the majority of the applied energy in metal deformation and the friction between tool and workpiece appear to enhance heat at the cutting area [1]. The heat generated at this area causes numerous economic and technical problems in the machining process. Some of these problems include rapid wear of the tool due to diffusion acceleration inducing of residual stresses and structural changes in the machined surface and the tool due to exerted thermal gradients, and also thermal distortion and deformation of the work piece, especially in thin-walled workpieces [2]. In order to attain optimal process outputs, it is important to identify creation manner, intensity, and heat distribution in the cutting area precisely. Despite many research projects done in this area; it is difficult to present a perfect theory of the heat generation mechanism and also to predict heat intensity and distribution in the machining process, due to the thermodynamic and nonlinear complex nature of this process, which also involves high pressure and strain in a small area [3].

Recently, there have been lots of unsolved issues in this area and some contradictory results have been reported from research projects. However, the influence of machining different pa-

rameters, material, and the geometry of the tool on the heat in the cutting area has been proved by many researchers [4-6]. Tool material is one of the effective parameters in cutting process efficiency and generated heat in the cutting area. In the machining of high strength aluminium alloys, cemented carbide tools are the most widely used tools. Among different metals, aluminium alloys have a suitable machinability due to a low machining force and low generated heat. Using common tool for machining these alloys creates built-up edge (BUE) which decreases tool-life and process efficiency especially in dry machining [7]. Therefore, using cutting tools with low friction and high hardness may lead to heat and BUE reduction and ultimately the tool's life, and process efficiency increase. Polycrystalline diamond (PCD) cutting tools are one of the most effective tools in aluminium alloys machining. PCD tools consist of an artificial diamond layer which is constructed at very high pressure and temperature and is brazed on a base of cemented carbide. These tools have unique characteristics including very high hardness, Young's modulus, and thermal conductivity, and a low friction coefficient of their surface which leads to enhance in cutting process effectiveness [8].

Experimental measurement and studying temperature in the cutting area are another challenge in machining science, and numerous methods have been developed for this. Several important methods use a thermocouple, infrared radiation (IR) measurement, measurement of hardness, and study of metal's microstructure changes which may provide some advantages or disadvantages [9]. One of the effective techniques of measuring temperature is infrared radiation measurement, which is a non-contact method. In this method, the temperature of the body is measured by considering the thermal energy or infrared radiation which is radiated from the body [10].

This research is aimed to study the effect of cutting parameters and tool material on the temperature of cutting area in turning of a thin walled workpiece which is made of aluminium alloy Al-7075. To measure temperature, a thermal infrared camera (IR) was used, and factors affecting the accuracy of measurements were evaluated.

2. Materials and methods

2.1 Infrared temperature measurement principle

Each hot object with a temperature higher than absolute zero (Kelvin's zero or $-273.15\text{ }^{\circ}\text{C}$) radiates an infrared radiation according to its temperature. The relation between radiated energy q_e , and an object's temperature is defined by Stefan Boltzmann law:

$$q_e = \varepsilon\sigma T^4 \quad (1)$$

Where σ is the Stefan Boltzmann constant and is equal to $\sigma = 5.67 \cdot 10^{-8} \left(\frac{\text{W}}{\text{m}^2\text{K}^4} \right)$. T is the thermodynamic temperature of an object in terms of K and ε is the emissivity coefficient of the object's surface. ε is defined as the emitted energy of a body at a specific temperature divided by the emitted energy of a black body, which is a dimensionless quantity. A black body is an object or material which absorbs the all existing radiations with any wave length and does not reflect any radiation [11]. An ideal black body theoretically has an emissivity coefficient of 1, but in practice, the emissivity coefficient of all objects is less than 1. When the thermal radiation collapses onto an object, it may be absorbed, reflected, or transmitted. The relation between absorptivity α , reflectivity ρ and transmissivity τ is defined as below

$$\alpha + \rho + \tau = 1 \quad (2)$$

In fact, the effective radiation received by the infrared detectors of an infrared thermal camera consists of three parts: (1) the object's radiation; (2) the radiation caused by light and the reflection of environmental heat on the object's surface and (3) atmospheric transmission radiation. Infrared detectors integrate radiation energy received in their working wavelength range, and then create its corresponding electrical signal $f(T_r)$:

$$f(T_r) = \tau_\alpha \varepsilon f(T) + \tau_\alpha (1 - \varepsilon) f(T_\mu) + (1 - \tau_\alpha) f(T_a) \quad (3)$$

This relation is a general equation for temperature measurement in a thermal camera in which τ_α is atmospheric transmissivity. T , T_r , T_μ and T_a are the measured temperature of the object, temperature shown by camera, environment temperature, and temperature of atmosphere respectively. The three right-hand side terms of the above equation define the object's radiation, the radiation caused by the reflection of object and radiation of atmospheric transmission, respectively. If the object is a black body, then: $\tau_\alpha = 1$ and therefore: $f(T_r) = f(T)$, meaning the temperature shown by the camera equals the object's temperature. But for any other object except a black body and especially for any metal with a high reflection and low absorptivity, there is a significant variation between $f(T_r)$ and $f(T)$. When the distance between the target object and the camera is small, then the effect of atmospheric radiation is negligible [12]. Thus, the accuracy of emissivity coefficient is the most important parameter in the accuracy of temperature measurement with an infrared thermal camera, since this parameter will fully specify the surface's characteristics in regard to absorptivity or the reflection of infrared radiation [13].

The IR method has many advantages; first, the IR method is a non-contact method and does not create any interference with heat flow in the cutting area. Also, the IR method has a very fast response. However, the IR technique has restrictions, such as the high dependency of measurement accuracy on the precise determination of the emissivity coefficient [14]. In some of the research performed on heat measurement with the IR technique, the emissivity coefficient of the tool and the workpiece is not mentioned, or the emissivity coefficient change of the machined surface and chip is not considered [15-17]. Some researchers have covered the surface of the workpiece or the tool with a material with a specific emissivity coefficient, to decrease the errors due to the determination of the emissivity coefficient [18, 19]. This method is applicable in the measurement of a fixed surface, but in machining, due to material removal, a new surface with a different emissivity coefficient will be created, and the reflection of the new surface on the covered surface and the chip surface decreases the effectiveness of this method.

2.2 Experimental procedure

Several different experiments were carried out on a thin-walled parts of Al-7075 alloy by a computer numerical control (CNC) machine (Tabriz TC50 model), to study the effects of various machining parameters on the heat generated in the cutting area. To evade the pressure of chuck jaws on the workpiece and its subsequent deformation, the workpiece was bolted on a fixture which was fastened into a chuck. Fig. 1 shows the geometry of the fixture, the workpiece and the assembled workpiece on the fixture.

The temperature was measured by using an IR camera (Dali DL700 model). The camera was mounted on a sheet which was linked to the turret, so that by using tool feed on the workpiece, the gap between the cutting area and the infrared camera remained constant. Fig. 2 shows the setup for performing the experimental case studies.

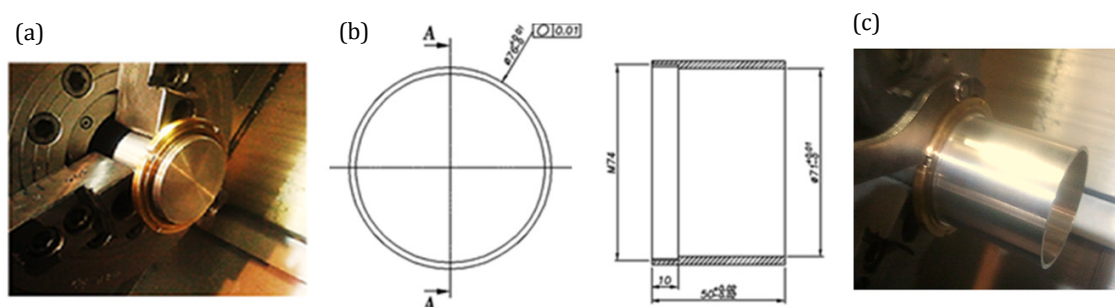


Fig. 1 The geometry of (a) the fixture, (b) the workpiece, (c) and the assembled workpiece on the fixture

The conditions of machining process

To study the effects of different conditions of the cutting process on the temperature, and the effect of various parameters on each other, a full factorial design was used for experimental case studies. This study investigates the effects of feed rate, cutting speed, and tool material.

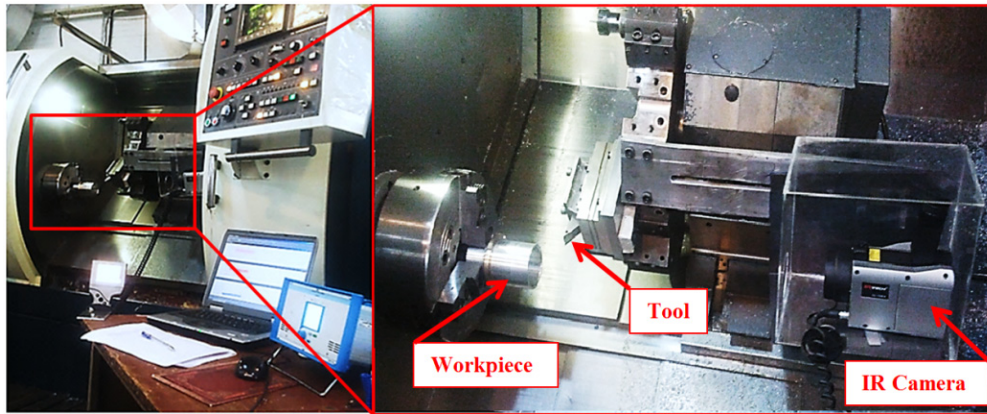


Fig. 2 The setup for measurement of the machining temperature in the CNC machine

Table 1 Machining parameters and required levels

Parameters	Level			
	A	B	C	D
Feed rate (mm/min)	60.0	120.0	180.0	-
Cutting speed (m/min)	230.0	350.0	470.0	590.0
Cutting tool	Polycrystalline diamond	Cemented carbide	-	-

Table 1 presents various levels for cutting parameters which were applied in case studies. Therefore, 24 tests were machined by using a CNC lathe machine. In order to validate the experimental results, each test was repeated three times. Moreover, in order to study the effect of the tool material on the temperature, two type of cutting insert with various materials of cemented carbide (Sandvik-VCGX160404-AL) and PCD (Sandvik-VCMW160404FP) were utilized. In the all experiments, the cutting depth equalled 1 mm in dry cutting condition.

Emissivity calibration and temperature measurement

To measure the heat in the cutting area, a thermal infrared camera was applied. The camera had a spectral range of 8-14 μm, a frame rate of 50/60 Hz and a temperature resolution of 0.05 °C. The camera’s detector was uncooled amorphous Silicon and sensitivity of 0.08 °C in 30 °C. The calibration of the camera’s detector was performed in different temperature ranges, using a black body (Optikos-model BBS-200). The black body’s emissivity was 0.994. Since, the 3.4 μm to 5 μm wavelength bandwidth provides higher accuracy in the machining process [20, 21], 4 μm wavelength bandwidth was adjusted in the camera. The camera lens which show a 15mm × 20 mm window were located on the cutting area to reach a 320 × 256 pixels resolution.

Emissivity is a function of temperature, wavelength, surface characteristics, and emission direction. However, the temperature is the most important factor influencing the emissivity as the luminance of a black body (L_{λ}^0) is a function of wavelength (λ) and temperature (T) in the Plank’s law:

$$L_{\lambda}^0 = \frac{C_1 \lambda^{-5}}{\pi \left[\exp\left(\frac{C_2}{\lambda T}\right) - 1 \right]} \tag{4}$$

C_1 and C_2 are constant parameters. In fact, the emissivity (ε) is defined as the ratio between the real monochromatic luminance and the luminance of a black body as below:

$$\varepsilon = \frac{L_{\lambda}(\lambda, T, \Delta)}{L_{\lambda}^0(\lambda, T)} \tag{5}$$

$L_{\lambda}(\lambda, T, \Delta)$ is defined as value of luminance for wavelength λ , at temperature T and direction Δ . The relation between luminance with wavelength and temperature is shown in Fig. 3(a). As this figure shows temperature is the most important factor which influences the emissivity coefficient [22]. Accurate determination of emissivity is the most important parameter in temperature

measurement accuracy with an infrared camera. The emissivity coefficient of a chip surface changes by varying temperature during machining. Since the aim of this research is measuring the temperature of the chip, to increase the accuracy, the precise determination of the chip's emissivity for different temperature ranges is necessary. Therefore, a part of the chip, were heated to different temperature ranges from 50-310 °C by using a tungsten element device which creates a controlled temperature by utilizing specified voltage and current. The exact value of chip's temperature was determined via a contact thermocouple (Testo model 925-T/C Type) and the chip's temperature was measured using the IR camera simultaneously. The emissivity of the IR camera was calibrated and defined so that the camera's apparent temperature was precisely identical with the thermocouple's measured temperature. Fig. 3(b) shows the results of experimentally emissivity extracted curve in different temperature ranges for Al-7075 according to above instruction. Results showed that by changing temperature from 50-310 °C the emissivity coefficient values were varied between 0.136 and 0.254. By following this instruction, the accurate emissivity of the chip for different temperature was extracted. Since the reflection of emitted radiation in the measurement environment on the desired object leads to an increase in its emitted radiation and therefore a decrease in measurement accuracy, the present research tried to eliminate all light and heat sources in the measurement area during the experiments.

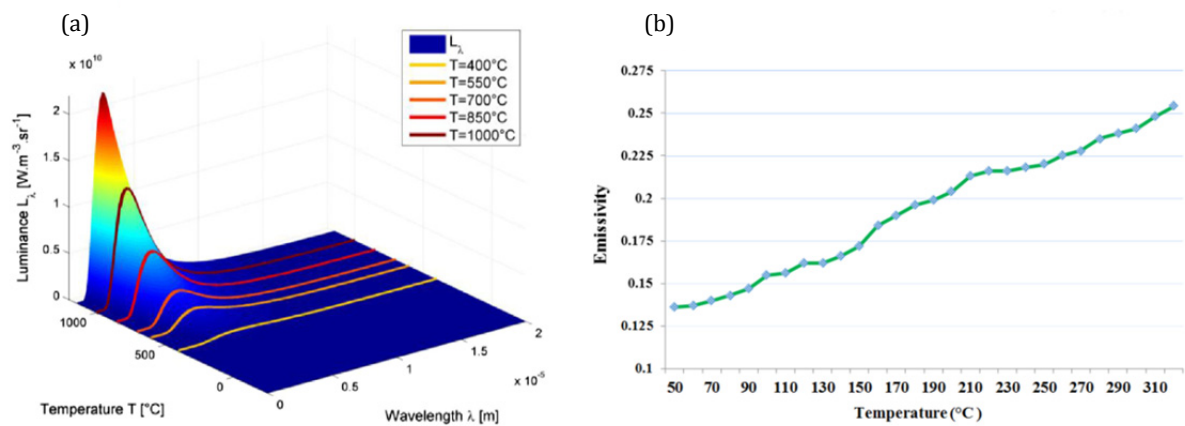


Fig. 3 (a) Luminance as a function of wavelength and temperature [22], (b) Experimental emissivity curve which is extracted for different temperatures for Al-7075

3. Results and discussion

Fig. 4 shows two thermal images of the cutting area which were achieved through experiments. Fig. 4(a) shows that the chips gather around the cutting area and the tool, while Fig. 4(b) indicates that the produced chips get away from cutting area. By comparing these two images, it can be observed how the increase of the emitted energy from a body is affected by reflection. Fig. 4(a) shows that due to the chip warping and aggregation around the tool, the camera's measured temperature increases significantly, so that in the same machining conditions, due to chip aggregation, 90 °C temperature difference was occurred. The reason is that each chip acts as a thermal radiation energy resource due to its high temperature. While hot chips are aggregated in a small area, reflected energy is emitted from every part of the chip to the other chips and continuing this procedure leads to an intensive and exponential increase of the infrared radiation emitted from the chip and ultimately increases the camera's calculated temperature.

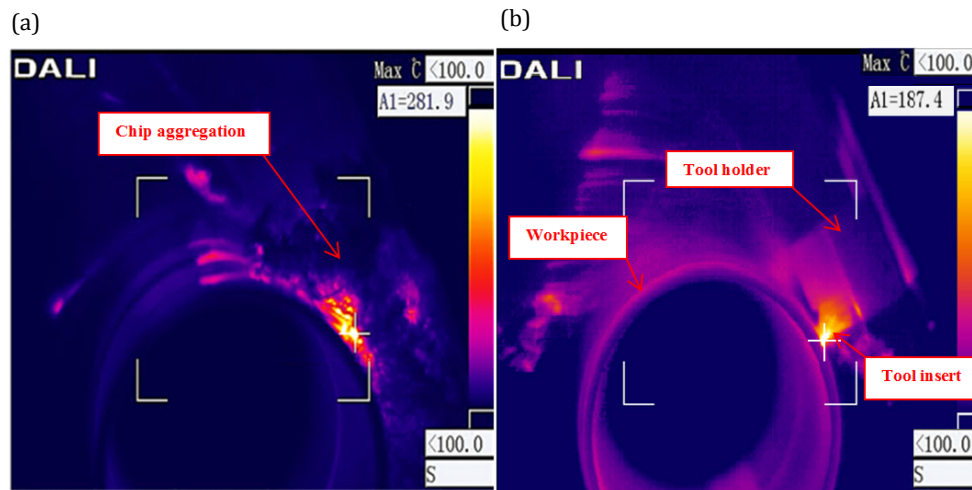


Fig. 4 Thermal infrared image in two cases of (a) chip aggregation and (b) appropriate expulsion of chip from cutting area

This process ultimately increases the camera's calculated temperature. Indeed, in the Eq. 3, $\tau_{\alpha}(1 - \varepsilon)f(T_{\mu})$ significantly increases which is related to the radiation reflected on the surface. Chip aggregation occurs for continuous chips, especially in the soft material and aluminium alloys machining. This issue was considered in the temperature measurement of the experimental case study to prevent inaccurate measurement. During the experiments, the temperature measured and recorded in the first 10 mm part of workpiece from starting point to prevent the possible errors due to the reflected energy emitted from the machined surface.

In the machining process, a part of the heat generated is transferred to the machined surface and the tool and makes a thermal gradient in the workpiece and tool which causes micro-structural changes in the metal, partial expansion, and induces residual stresses [2]. Fig. 5 shows that the thermal gradient applied to the workpiece. As this figure shows, in both image (a) and image (b), the cross-hair indicates a thermal gradient in the inner surface of the workpiece and the region of tool contact with the workpiece. In these areas, the temperature in a thin band is significantly superior to the other sections. This phenomenon is more intensive in metals such as aluminium with higher heat transfer coefficient; because heat transfers to beneath the surfaces of the workpiece rapidly. This intensive thermal gradient is created in some seconds in a section of the workpiece which leads to partial expansion and residual stresses in the workpiece. This effect is especially important in thin-walled workpieces as the induced residual stresses lead to dimensional instability and distortion.

Fig. 5 indicates that by increasing the temperature of the cutting area, a thermal gradient be transferred to the workpiece increases. Image (a) corresponds to an experiment when feed rate and cutting speed are 180 mm/min and 590 m/min respectively, for the carbide tool. The measured temperature in this test was 202 °C. Image (b) for the PCD tool corresponds to an experiment when the feed rate and cutting speed are 120 mm/min and 590 m/min, respectively. The reported temperature in this case was 132 °C. Due to the greater heat generation in Fig. 5(a) in comparison with (b), the heat transferred to the surface of the workpiece is much higher.

Figs. 6(a) and (b) indicate the experimental results which show the effect of feed rate and cutting speed on the measured temperature of chip for carbide and PCD tools in 2D and 3D plots, respectively. The temperature of the chip in the PCD tool is significantly lower than in the carbide tools. Nevertheless, by increasing feed rate and cutting speed the temperature increases and the heat increase slope becomes steeper as the cutting speed raises for both PCD and Carbide tools. For instance, when feed rate and cutting speed are 180 mm/min and 590 m/min, respectively, the maximum temperature for the PCD insert is 149 °C, while maximum measured temperature for the carbide insert is 203 °C.

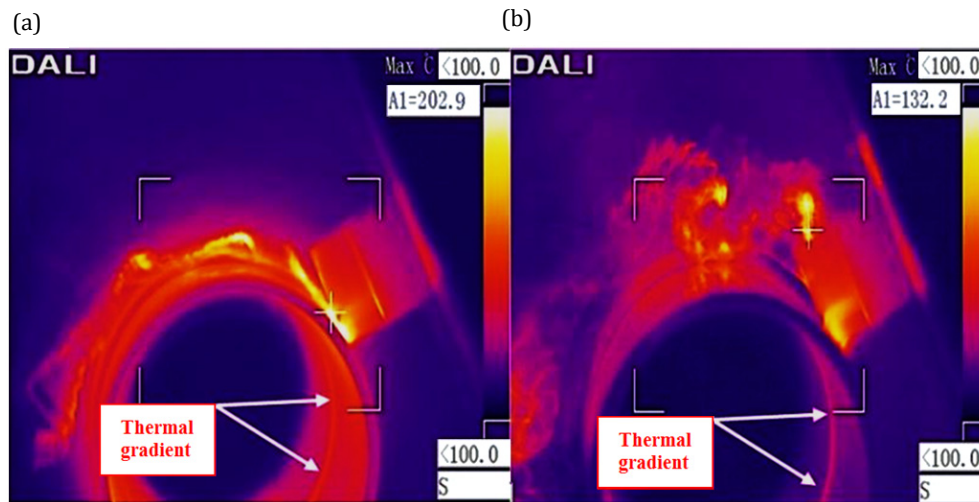


Fig. 5 The transmission of the generated heat from cutting zone to the workpiece, and the creation of a thermal gradient in a section of the workpiece

Generally, PCD insert has lower friction coefficient in comparison to carbide tools [23]. Therefore, heat caused by friction in rake and flank surfaces will be lower. Moreover, due to the friction being lower the required forces to form chips decrease and thus less heat is generated in the cutting area. Fig. 7 shows the microscopic images of the rake surfaces of two PCD and carbide tools at a magnification of 400 times. As seen in this figure, the surface of PCD tools has a more uniform structure and fewer ups and downs than the surface of carbide tools, which reduce the coefficient of friction in PCD tools.

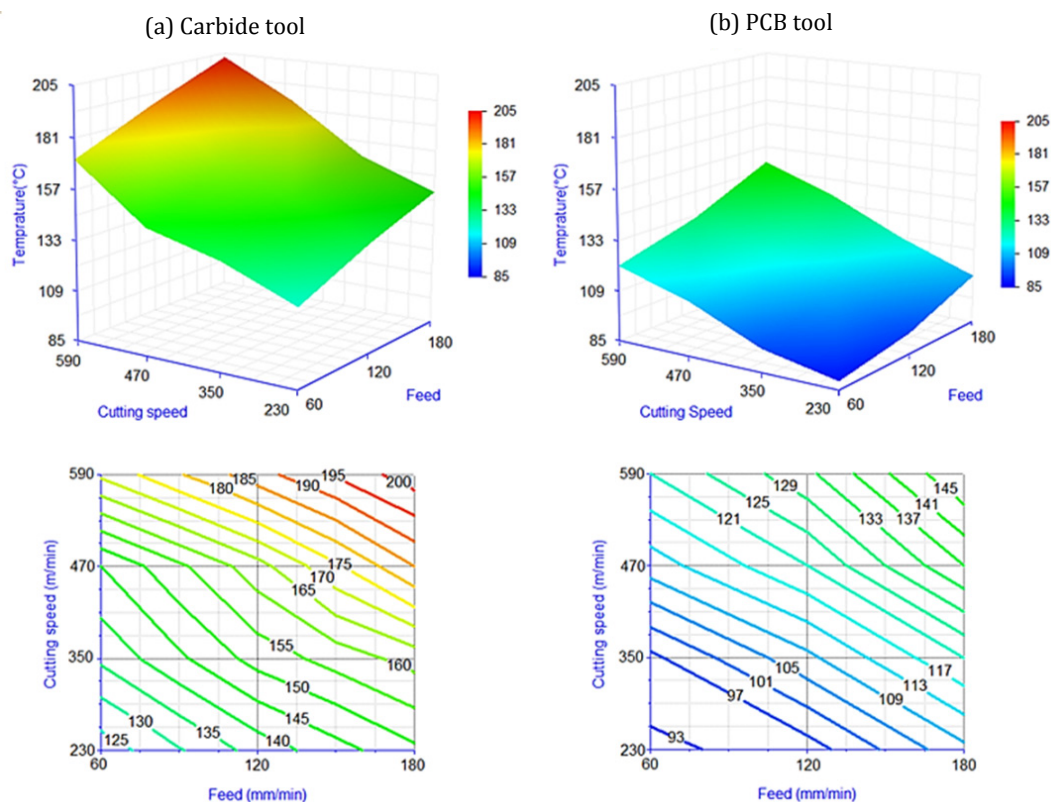


Fig. 6 Experimental results of measured chip temperature for carbide tool (a) and PCD tool (b) versus feed rate and cutting speed changes

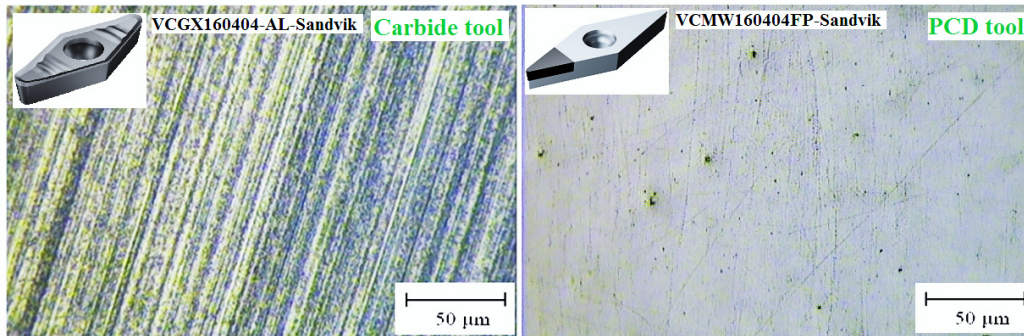


Fig. 7 Microscopic image: Rake surface of PCD and carbide tools in experiments with a magnification of 400×

Another characteristic of PCD tools is a higher thermal conductivity in comparison with carbide tools, which leads to more heat transfer from the cutting area and thus a decrease in the temperature of the chip and workpiece [23]. On the other hand, because less heat and a lower machining force are applied to the tool, and because of the high strength and hardness of PCD tools, the rate of wear is much slower than it is for carbide tools. Therefore, the temperature increase of the cutting area due to tool wear in these tools is much lower than that of carbide tools. In general, using PCD tools in high-strength aluminium alloys machining is preferable to using carbide tools and increases cutting efficiency.

Fig. 8 shows that to study the effect of emissivity coefficient on the accuracy of the temperature measurement value. In this figure the measured temperature values with calibrated emissivity are compared to the temperature values with a constant emissivity, 0.11, according to reference [24]. As can be seen, by increasing temperature, the difference between the measured values increases. The reason for this result is that in the high measured temperature, the difference between the constant and calibrated emissivity coefficients is more. By using the constant emissivity, 0.11, which is less than all the calibrated emissivity values, the measured temperature by IR camera increases, which is in accordance with Eq. 3. Based on the achieved results, the lowest and highest difference values which are measured at the same condition are 5 °C and 45 °C, respectively, and the average temperature difference is 20.5 °C. These results clearly show the importance of precise calibration of chip’s emissivity for different temperature ranges in temperature measurement by infrared imaging in machining processes.

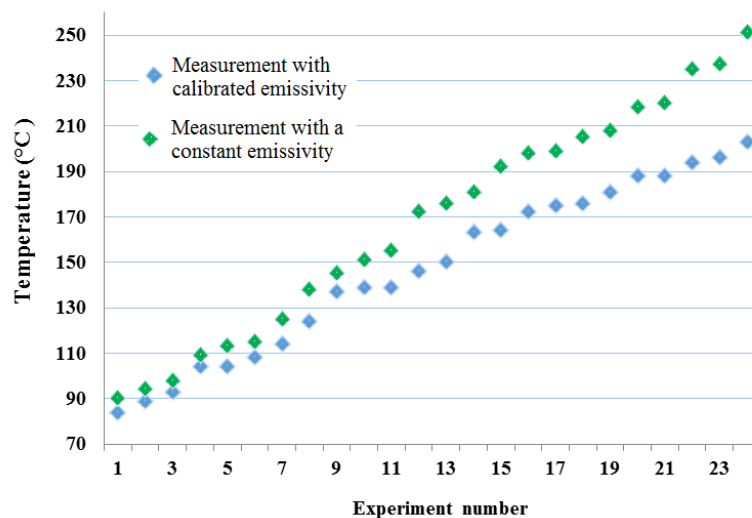


Fig. 8 Comparison between the measured temperatures values with the calibrated emissivity and a constant emissivity (0.11)

4. Conclusion

In the present study, the influence of cutting parameters and tool material on the temperature of the cutting area in the turning of an Al-7075 alloy thin-walled workpiece were investigated. To measure temperature, a thermal infrared camera (IR) was used, and factors affecting the accuracy of measurements were evaluated. The results showed that using IR camera is one of the effective methods for temperature measurement in machining processes. However, due to limitations in the IR method, some remarks should be considered to increase the validity and accuracy of temperature measurement in the machining processes. One of the effective parameters in the temperature measurement by using thermal imaging is defining and calibrating a precise emissivity for different ranges of temperature which are investigated in the present paper by performing experimental tests. The achieved results indicate that the lack of calibration of emissivity coefficient cause a considerable difference between the measured values and leads to errors as high as 24 % in temperature measurement.

The results also showed that chip aggregation in the cutting area due to the reflection of emitted energy between hot chips can cause huge errors in temperature measurement which should be considered. The studied experiments that used the IR camera clearly indicated the transition a portion of the generated heat to the workpiece and consequently forming a thermal gradient on it. The thermal gradient created in the thin-walled workpiece can cause various problems such as metal micro-structural change, partial expansion, residual stresses, and distortion which may be prevented by using temperature-reducing techniques.

According to the results obtained in the cutting process with the PCD insert, due to the low friction coefficient and improved cutting conditions of this tool, the temperature in cutting areas was much lesser than that of the carbide insert. In cutting experiments with the PCD insert, the average temperature was 71 % lesser than in the carbide insert. Therefore, PCD inserts are an appropriate substitute for carbide inserts in the cutting of high-strength aluminium alloys. From the results of this research, it can be concluded that the temperature generated in the cutting area can be lowered significantly by using PCD tools and selecting appropriate machining parameters. Therefore, the results of this research create a more comprehensive perception of the operation and effectiveness of PCD tools in machining of different alloys.

References

- [1] Wang, Z., Basu, S., Saldana, C. (2017). Low-temperature machining in a fully submerged cryogenic environment, *Machining Science and Technology*, Vol. 21, No. 1, 19-36, doi: [10.1080/10910344.2016.1260428](https://doi.org/10.1080/10910344.2016.1260428).
- [2] Masoudi, S., Amirian, G., Saeedi, E., Ahmadi, M. (2015). The effect of quench-induced residual stresses on the distortion of machined thin-walled parts, *Journal of Materials Engineering and Performance*, Vol. 24, No. 10, 3933-3941, doi: [10.1007/s11665-015-1695-7](https://doi.org/10.1007/s11665-015-1695-7).
- [3] Riou, O., Guiheneuf, V., Delaleux, F., Logerais, P.-O., Durastanti, J.-F. (2016). Accurate methods for single-band apparent emissivity measurement of opaque materials, *Measurement*, Vol. 89, 239-251, doi: [10.1016/j.measurement.2016.04.006](https://doi.org/10.1016/j.measurement.2016.04.006).
- [4] Thepsonthi, T., Özel, T. (2015). 3-D finite element process simulation of micro-end milling Ti-6Al-4V titanium alloy: Experimental validations on chip flow and tool wear. *Journal of Materials Processing Technology*, Vol. 221, 128-145, doi: [10.1016/j.jmatprotec.2015.02.019](https://doi.org/10.1016/j.jmatprotec.2015.02.019).
- [5] Heigel, J.C., Whinton, E., Lane, B., Donmez, M.A., Madhavan, V., Moscoso-Kingsley, W. (2017). Infrared measurement of the temperature at the tool-chip interface while machining Ti-6Al-4V, *Journal of Materials Processing Technology*, Vol. 243, 123-130, doi: [10.1016/j.jmatprotec.2016.11.026](https://doi.org/10.1016/j.jmatprotec.2016.11.026).
- [6] Jiang, F., Liu, Z., Wan, Y., Shi, Z., Zhang, H. (2016). Experimental investigation of cutting tool temperature during slot milling of AerMet 100 steel, *Proceedings of the Institution of Mechanical Engineers, Part B: Journal of Engineering Manufacture*, Vol. 230, No. 5, 838-847, doi: [10.1177/0954405414563421](https://doi.org/10.1177/0954405414563421).
- [7] Tabei, A., Shih, D.S., Garmestani, H., Liang, S.Y. (2016). Micro-texture evolution in aggressive machining of al alloy 7075, *Materials and Manufacturing Processes*, Vol. 31, No. 13, 1709-1717, doi: [10.1080/10426914.2015.1090597](https://doi.org/10.1080/10426914.2015.1090597).
- [8] Amini, S., Khosrojerdi, M.R., Nosouhi, R., Behbahani, S. (2014). An experimental investigation on the machinability of Al₂O₃ in vibration-assisted turning using PCD tool, *Materials and Manufacturing Processes*, Vol. 29, No. 3, 331-336, doi: [10.1080/10426914.2013.864411](https://doi.org/10.1080/10426914.2013.864411).
- [9] Davoodi, B., Hosseinzadeh, H. (2012). A new method for heat measurement during high speed machining, *Measurement*, Vol. 45, No. 8, 2135-2140, doi: [10.1016/j.measurement.2012.05.020](https://doi.org/10.1016/j.measurement.2012.05.020).

- [10] Yashiro, T., Ogawa, T., Sasahara, H. (2013). Temperature measurement of cutting tool and machined surface layer in milling of CFRP, *International Journal of Machine Tools and Manufacture*, Vol. 70, 63-69, doi: [10.1016/j.ijmachtools.2013.03.009](https://doi.org/10.1016/j.ijmachtools.2013.03.009).
- [11] Svetlitzka, A., Slavenko, M., Blank, T., Brouk, I., Stolyarova, S., Nemirovsky, Y. (2014). THz measurements and calibration based on a blackbody source. *IEEE Transactions on Terahertz Science and Technology*, Vol. 4, No. 3, 347-359, doi: [10.1109/TTHZ.2014.2309003](https://doi.org/10.1109/TTHZ.2014.2309003).
- [12] Quan, Y., Xu, H., Ke, Z. (2011). Research on some influence factors in high temperature measurement of metal with thermal infrared imager, *Physics Procedia*, Vol. 19, 207-213, doi: [10.1016/j.phpro.2011.06.150](https://doi.org/10.1016/j.phpro.2011.06.150).
- [13] Liu, D., Wang, G., Nie, Z., Rong, Y.K. (2016). An in-situ infrared temperature-measurement method with back focusing on surface for creep-feed grinding, *Measurement*, Vol. 94, 645-652, doi: [10.1016/j.measurement.2016.09.013](https://doi.org/10.1016/j.measurement.2016.09.013).
- [14] Müller, B., Renz, U. (2003). Time resolved temperature measurements in manufacturing, *Measurement*, Vol. 34, No. 4, 363-370, doi: [10.1016/j.measurement.2003.08.009](https://doi.org/10.1016/j.measurement.2003.08.009).
- [15] Hou, J., Zhao, N., Zhu, S. (2011). Influence of cutting speed on flank temperature during face milling of magnesium alloy, *Materials and Manufacturing Processes*, Vol. 26, No. 8, 1059-1063, doi: [10.1080/10426914.2010.536927](https://doi.org/10.1080/10426914.2010.536927).
- [16] Hamlaoui, N., Azzouz, S., Chaoui, K., Azari, Z., Yaltese, M.-A. (2017). Machining of tough polyethylene pipe material: Surface roughness and cutting temperature optimization, *The International Journal of Advanced Manufacturing Technology*, Vol. 92, No. 5-8, 2231-2245, doi: [10.1007/s00170-017-0275-4](https://doi.org/10.1007/s00170-017-0275-4).
- [17] Cuesta, M., Aristimuño, P., Garay, A., Arrazola, P.J. (2016). Heat transferred to the workpiece based on temperature measurements by IR technique in dry and lubricated drilling of Inconel 718, *Applied Thermal Engineering*, Vol. 104, 309-318, doi: [10.1016/j.applthermaleng.2016.05.040](https://doi.org/10.1016/j.applthermaleng.2016.05.040).
- [18] Vitkovskii, V.V., Gorshenev, V.G., Potapov, Y.F. (2009). Measurement of spectral directional emissivity of materials and coatings in the infrared region of spectrum, *Thermal engineering*, Vol. 56, No. 3, 245-248, doi: [10.1134/S0040601509030100](https://doi.org/10.1134/S0040601509030100).
- [19] Armendia, M., Garay, A., Villar, A., Davies, M.A., Arrazola, P.J. (2010). High bandwidth temperature measurement in interrupted cutting of difficult to machine materials, *CIRP Annals, Manufacturing Technology*, Vol. 59, No. 1, 97-100, doi: [10.1016/j.cirp.2010.03.059](https://doi.org/10.1016/j.cirp.2010.03.059).
- [20] Meca Meca, F.J., Rodríguez Sanchez, F.J., Sanchez, P.M. (2002). Calculation and optimisation of the maximum uncertainty in infrared temperature measurements taken in conditions of high uncertainty in the emissivity and environment radiation values, *Infrared Physics & Technology*, Vol. 43, No. 6, 367-375, doi: [10.1016/S1350-4495\(02\)00125-1](https://doi.org/10.1016/S1350-4495(02)00125-1).
- [21] Boué, C., Holé, S. (2012). Infrared thermography protocol for simple measurements of thermal diffusivity and conductivity, *Infrared Physics & Technology*, Vol. 55, No. 4, 376-379, doi: [10.1016/j.infrared.2012.02.002](https://doi.org/10.1016/j.infrared.2012.02.002).
- [22] Valiorgue, F., Brosse, A., Naisson, P., Rech, J., Hamdi, H., Bergheau, J. M. (2013). Emissivity calibration for temperatures measurement using thermography in the context of machining, *Applied Thermal Engineering*, Vol. 58, No. 1-2, 321-326, doi: [10.1016/j.applthermaleng.2013.03.051](https://doi.org/10.1016/j.applthermaleng.2013.03.051).
- [23] Li, G., Rahim, M.Z., Ding, S., Sun, S. (2016). Performance and wear analysis of polycrystalline diamond (PCD) tools manufactured with different methods in turning titanium alloy Ti-6Al-4V, *The International Journal of Advanced Manufacturing Technology*, Vol. 85, No. 1-4, 825-841, doi: [10.1007/s00170-015-7949-6](https://doi.org/10.1007/s00170-015-7949-6).
- [24] Wen, C.-D., Mudawar, I. (2006). Modeling the effects of surface roughness on the emissivity of aluminum alloys, *International Journal of Heat and Mass Transfer*, Vol. 49, No. 23-24, 4279-4289, doi: [10.1016/j.ijheatmasstransfer.2006.04.037](https://doi.org/10.1016/j.ijheatmasstransfer.2006.04.037).